Metastability of heavy lanthanides in the ZnO wurtzite structure

Eugenio Hernán Otal [a,b,*], Songhak Yoon [a], Myriam Aguirre [a], Anke Weidenkaff [a]

[a] EMPA, Swiss Federal Laboratories for Materials Testing and Research, Solid State Chemistry and Catalysis, Ueberlandstr. 129, CH-8600 Dübendorf, Switzerland
[b] CINSO, Centro de Investigaciones en Sólidos, CONICET, CITEFA, San Juan Bautista de La Salle 4397, (B1603ALO) Villa Martelli, Buenos Aires, Argentina

ARTICLE INFO

ABSTRACT

The introduction and stability of the heavy lanthanide Er, into ZnO was studied by HRTEM, XRD and thermal treatments. The applied synthesis route allows introducing the Er atoms in the lattice in a metastable state. The stability depends on the Er concentration. ZnO with Er concentrations of less than 2% are stable up to 800 °C, while higher concentrations result in a phase segregation at $T > 700$ °C. Unit cell parameters obtained from the Rietveld refinement of XRD patterns provide a conclusive evidence of the incorporation of the Er ions in the host ZnO matrix.

© 2011 Elsevier B.V. All rights reserved.

1. Introduction

ZnO is a II–VI semiconductor with extraordinary optical and electrical properties. Its environmentally friendly and nanostructured material can easily be obtained in soft-chemistry processes using polar solvents. It crystallizes in a hexagonal crystal structure with $P6_3mc$ space group, and shows anisotropic growth leading to a wide variety of shapes like needles, tetrapods, nanorods, shells, ribbons, and highly faceted rod shapes [1].

Lanthanide-doped ZnO has increasingly been used in varistors [2] due to its excellent nonlinearity in I–V response, and in optical devices owing to its luminescence [3].

Recently, ZnO attracted the research community's attention because of the potential use in thermoelectric (TE) converters. One of the most studied system is ZnO:Al [4,5]. Al doping leads to an improvement of the electrical conductivity, but the high thermal conductivity is still a drawback. One way to reduce the thermal conductivity is the introduction of heavy atoms, for example lanthanides (Ln) [6]. Substitutions with lanthanides reduce the thermal conductivity of the samples in two aspects: first, they serve as heavy atom impurities enhancing the scattering of phonons in the lattice. The second aspect is related to its 4f electronic levels. The crystal field splitting in these levels is weak. Thus, the difference in energy between two levels is in the order of the lattice phonon energy. In this case, the phonons are absorbed and re-emitted in arbitrary directions, reducing the thermal conductivity, which is favorable for TE converters [7].

Previous studies showed that the introduction of Ln in the ZnO matrix is not easily achieved by direct solid state reactions of the oxides [8,9] or by combustion methods [10]. The motivation of this work is to increase the understanding of Er introduction in the lattice and the resulting influence on optical and electrical properties. The cationic substitution in the ZnO lattice or the segregation of Ln_2O_3 in grain boundaries determines in different ways the optical and electrical properties.

In this work, we followed a soft chemistry route for the synthesis. The quantitative analysis of the lanthanides incorporation was performed by ICP–OES (inductive coupled plasma–optical emission spectroscopy). Structural studies were done by HRTEM (High resolution transmission electron microscopy) and XRD (X-ray diffraction) which provided a conclusive evidence of Er introduction in ZnO and the stability of the system.

2. Experimental

2.1. Materials

Zinc acetate dihydrate (puriss.) (ZAD), Erbium acetate hydrate ($Er(AcO)_3 \cdot 8H_2O$) (99.9%) (Sigma–Aldrich), potassium hydroxide hydrate (p.a.) (KOH), absolute ethanol (EtOH) (p.a.) (Merck), dimethylformamide (DMF) (p.a.) (J.T. Baker), Hexane (p.a.) (Riedel-de Haen) were used without further purification. The water of crystallization of the doping precursors was quantified by thermogravimetric analysis (TGA). The precursor decomposition and conversion into the oxide was performed by heating the acetates in air up to 1000 °C.

2.2. Sample preparation

The chosen synthetic route is a modified adaption of the procedure reported by Schwartz et al. [11]. In our route colloidal nanocrystalline ZnO was synthesized at

* Corresponding author at: EMPA, Swiss Federal Laboratories for Materials Testing and Research, Department of Solid State Chemistry, Ueberlandstrasse 129, 8600 Dübendorf, Zürich, Switzerland.
E-mail address: eugenio.otal@empa.ch (E.H. Otal).

room temperature by the addition of an ethanolic solution of KOH to ZAD dissolved in DMF. The ethanolic solution was prepared dissolving 0.93 g of KOH in 30 ml of EtOH by ultrasonication during 15 min to obtain a clear solution with a concentration of 0.552 mol/L. The DMF solution was obtained by dissolution of 1.99 g ZAD and a corresponding mass of lanthanide acetates in 90 mL (0.101 mol/L) under stirring. The basic solution was added dropwise with a rate of approximately 2 mL/min to the DMF solution under constant stirring. Rare earth doping was achieved by addition of $Er(AcO)_3 \cdot 8H_2O$ to the $Zn(AcO)_2 \cdot 2H_2O$ precursor solution. Nanocrystals prepared in this way precipitate from the DMF by addition of ethyl acetate. To eliminate remaining salts and impurities the nanoparticles were re-suspended in ethanol and re-precipitated with hexane. The obtained nanoparticles were dried at 130 °C over night, and thermally treated at 500 °C, 600 °C, 700 °C, 800 °C and 900 °C for 1 h.

Samples for transmission electron microscopy studies were prepared directly from the ethanolic suspension and deposited on a holey carbon copper grid. Images were obtained with a Phillips CM30 at 300 kV.

Powder X-ray diffraction (PXRD) patterns were obtained in a Bragg–Brentano geometry using a PANalytical XiPert PRO θ–2θ scan system. The incident X-Rays had a wavelength of 1.5406 (Cu Kα1). The diffraction patterns were scanned from 20° to 120° (2θ) with an angular step interval of 0.0167°. XRD patterns have been analyzed by the Rietveld refinement program, *Fullprof* [12], to determine the unit cell parameter. Thompson-Cox-Hastings (TCH) pseudo-Voigt functions were chosen as profile function among all the profiles in the *Fullprof* program [13].

3. Results and discussion

3.1. Quantitative elemental analysis

The samples were obtained from a wet chemistry precipitation route. In contrast to combustion or ceramic synthesis methods it has to be ensured that the doping elements do not remain in solution during the nanoparticle formation. Thus, a validation of Er incorporation was performed by ICP–OES. This method offers a better accuracy than EDS method (energy-dispersive X-ray spectroscopy) in the range of Er concentrations.

Fig. 1 shows the Er incorporated as a function of the nominal concentration. The introduction was deficient with a nonlinear behavior which can be related to the equilibrium between the ions in solution and the surface of the particles during the nanoparticles formation.

3.2. Transmission electron microscopy

The TEM micrograph of the obtained particles without thermal treatment is shown in Fig. 2. The shape of the nanoparticles is predominantly spherical and presents a narrow dispersion in the size distribution with a media around 10 nm. The nanoparticles also present a high crystallinity even in the case when no thermal treatment is performed. No evidence of Er segregated phases was found in these samples.
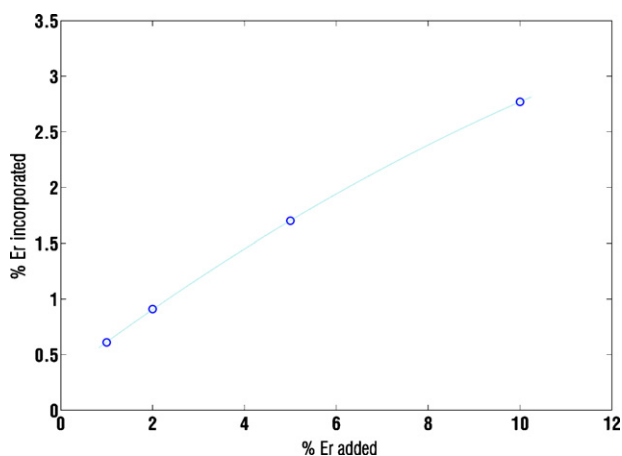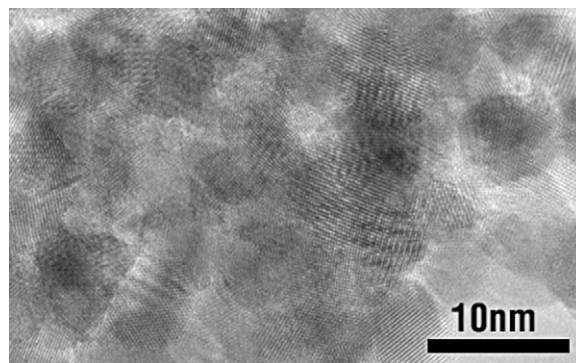

Fig. 2. HRTEM micrographs of ZnO:Er (2% nominal) nanoparticles obtained by a sol–gel method without thermal treatment.
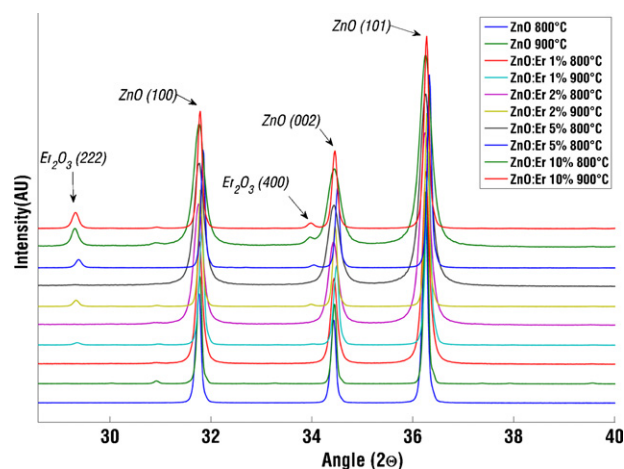

Fig. 3. XRD patterns of ZnO and ZnO:Er with different nominal concentration and thermal treatments. Samples are named according to its nominal composition.

3.3. X-ray diffraction

The PXRD data confirms the wurtzite structure to be the major phase of the synthesized ZnO and ZnO:Er samples, irrespective of the different thermal treatment, as majority phase (Fig. 3).

For samples with 1–5% nominal Er doping (less than 2% incorporated), PXRD showed single phase up to 800 °C, implying no Er_2O_3 phase segregation. Samples calcined at 900 °C reveal Er_2O_3 segregation. For 10% nominal Er doped ZnO (more than 2% incorporated), no phase segregation took place at $T < 700$ °C, but the Er_2O_3 phase can clearly be seen at $T > 800$ °C (Fig. 3).

The dependence of the unit cell parameters on Er doping obtained by Rietveld refinement of the PXRD patterns is shown in Fig. 4. The Er incorporation has a clear influence on the unit cell parameters of the ZnO. As the Er concentration increases, the *a*-axis increases while the *c*-axis simultaneously decreases.

The change of the cell parameters with the Er doping, and the lack of phase segregation at lower calcination temperatures ($T < 700$ °C), confirms the incorporation of Er in the ZnO structure. The increase of *a* parameter and the decrease of *c* axis could be an indicator that Er is not substituting Zn atoms. A simple Er for Zn substitution would be expected to result in an isotropic increase of the cell parameters. Thus, an interstitial position might be postulated for the Er atoms in the ZnO lattice.

3.4. Thermal stability

The sintering process consists in several processes, mainly densification and grain growth of the material. Among these processes,
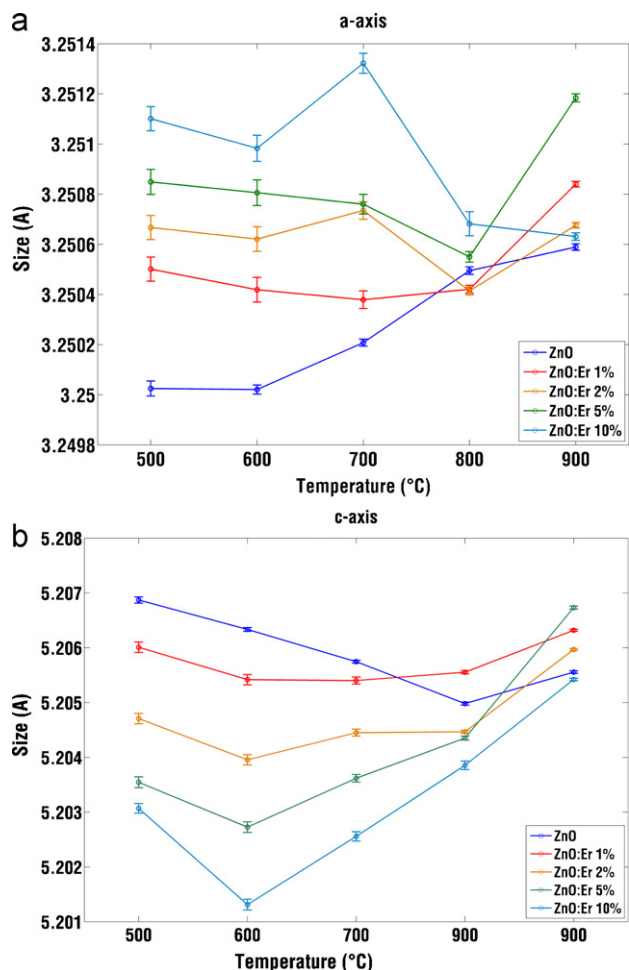

Fig. 1. Quantification of Er incorporated in the nanoparticles. The dashed line is a guideline to observe the nonlinear behavior.

Fig. 4. *a*-axis and *c*-axis obtained from Rietveld refinement of XRD patterns. Samples are named according to its nominal composition.

diffusion consists of mass transport and rearrange at atomic level [14]. The start temperature of the sintering process was empirically found to be 0.8–0.9 T_f (melting point) for a microcrystalline system, but for nanocrystalline materials this temperature is drastically decreased to 0.4–0.5 T_f [15,16].

In the studied ZnO system ($T_f^{ZnO} = 2248$ K), the phase segregation occurs in a temperatures range of around 1073–1173 K (800–900 °C), which approximately coincides with 0.5 T_f and the behavior of a nanocrystalline system.

According to these results the phase segregation can be attributed to the massive mass transport in the solid at the onset of the sintering temperature. This rearrangement settles the system in a thermodynamically more stable state, which is the segregated phase instead of the ZnO lattice with incorporated Er atoms.

4. Conclusions

A soft chemistry synthesis method for the production of ZnO:Er with good crystallinity and without Er_2O_3 phase segregation was developed. TEM studies proof the good quality of the crystalline homogeneous and single phase nanoparticles. No evidence of phase segregation was observed after thermal treatment at $T < 800$ °C for the samples with up to 2% Er doping, and at $T < 700$ °C for samples with more than 2% Er incorporated. The unit cell parameters derived by Rietveld refinements clearly indicates the dependence from the doping concentration: as the Er concentration increases (at a constant temperature) the *c*-axis is decreased and the *a*-axis increased. The influence of the Er concentration on the cell parameters and the absence of phase segregations at lower calcination temperatures confirm the introduction of Er into the ZnO structure.

References

[1] A. Djurišić, Y.H. Leung, Small 2 (2006) 944–961.
[2] D.R. Clarke, J. Am. Ceram. Soc. 82 (2004) 485–502.
[3] M. Abdullah, T. Morimoto, K. Okuyama, Adv. Funct. Mater. 13 (2003) 800–804.
[4] T. Tsubota, M. Ohtaki, K. Eguchi, H. Arai, J. Mater. Chem. 8 (1998) 409–412.
[5] T. Tsubota, M. Ohtaki, K. Eguchi, H. Arai, J. Mater. Chem. 7 (1997) 85–90.
[6] G.S. Nolas, M. Kaeser, R.T. Littleton, T.M. Tritt, Appl. Phys. Lett. 77 (2000) 1855.
[7] K. Berggold, M. Kriener, P. Becker, M. Benomar, M. Reuther, C. Zobel, T. Lorenz, Phys. Rev. B 78 (2008) 134402.
[8] L. Hongyu, K. Hui, J. Dongmei, S. Wangzhou, M. Xueming, J. Rare Earths 25 (2007) 120–123.
[9] Y. Inoue, Y. Okamoto, J. Morimoto, J. Mater. Sci. 43 (2007) 368–377.
[10] H. Han, L. Yang, Y. Liu, Y. Zhang, Q. Yang, Opt. Mater. 31 (2008) 338–341.
[11] D.A. Schwartz, N.S. Norberg, Q.P. Nguyen, J.M. Parker, D.R. Gamelin, J. Am. Chem. Soc. 125 (2003) 13205–13218.
[12] J. Rodríguez-Carvajal, Phys. B: Condens. Matter 192 (1993) 55–69.
[13] P. Thompson, D.E. Cox, J.B. Hastings, J. Appl. Crystallogr. 20 (1987) 79–83.
[14] J. Philibert, Atom Movements: Diffusion and Mass Transport in Solids, L'Editeur: EDP Sciences, 1991.
[15] P. Chen, I. Chen, J. Am. Ceram. Soc. 79 (1996) 3129–3141.
[16] P. Chen, I. Chen, J. Am. Ceram. Soc. 80 (2005) 637–645.